OPTIMAL CONVERGENCE OF THE ORIGINAL DG METHOD ON SPECIAL MESHES FOR VARIABLE TRANSPORT VELOCITY*

BERNARDO COCKBURN[†], BO DONG[‡], JOHNNY GUZMÁN[‡], AND JIANLIANG QIAN[§]

Abstract. We prove optimal convergence rates for the approximation provided by the original discontinuous Galerkin method for the transport-reaction problem. This is achieved in any dimension on meshes related in a suitable way to the possibly variable velocity carrying out the transport. Thus, if the method uses polynomials of degree k, the L^2-norm of the error is of order $k+1$. Moreover, we also show that, by means of an element-by-element postprocessing, a new approximate flux can be obtained which superconverges with order $k+1$.

Key words. discontinuous Galerkin methods, convection-reaction equation, error estimates

AMS subject classifications. 65N30, 65M60

DOI. 10.1137/080740805

1. Introduction. We prove *optimal* convergence properties of the original discontinuous Galerkin (DG) [16, 13] method for the convection-reaction problem

$$\nabla \cdot (\boldsymbol{\beta}\, u) + c\, u = f \quad \text{in } \Omega, \tag{1.1a}$$

$$u = g \quad \text{on } \Gamma^-. \tag{1.1b}$$

Here $\Omega \subset R^d$ is a bounded polyhedral domain, $\Gamma^- := \{x \in \partial\Omega : \boldsymbol{\beta} \cdot \boldsymbol{n}(x) < 0\}$, and $\boldsymbol{n}(x)$ is the outward unit normal at the point $x \in \partial\Omega$. The functions f and g are smooth, c is a bounded function, and, more importantly, $\boldsymbol{\beta}$ is a *smooth* function whose divergence is *not* necessarily equal to zero.

Let us describe our result. It is well known that, for *constant* transport velocities $\boldsymbol{\beta}$, the DG method for the above problem provides approximations converging with *suboptimal* rates on general meshes. This was shown for the first time in [14] for a particular type of two-dimensional mesh. The class of meshes for which this suboptimal rate of convergence can be demonstrated was recently extended in [17] to include some two-dimensional smooth, periodically varying meshes. On the other hand, in a diametrically opposed effort, a class of special multidimensional meshes for which the *optimal* order of convergence is actually achieved was recently uncovered in [6]. Here, we continue this effort and prove that a similar result also holds for *variable* transport velocities $\boldsymbol{\beta}$.

The variable velocities $\boldsymbol{\beta}$ we consider satisfy the following conditions:
(A1) $\boldsymbol{\beta}$ has no closed curves and $\|\boldsymbol{\beta}(\boldsymbol{x})\| \neq 0$ for every $\boldsymbol{x} \in \Omega$.
(A2) $\inf_{x \in \Omega}(c(\boldsymbol{x}) + \frac{1}{2}\nabla \cdot \beta(\boldsymbol{x})) \geq 0$.

See Ayuso and Marini [1]. For these velocities, we show that, for a *special* class of triangulations $\mathcal{T}_h$,

$$\| u - u_h \|_{L^2(\mathcal{T}_h)} + \| \partial_{\boldsymbol{\beta}} u - \partial_{\boldsymbol{\beta},h} u_h \|_{L^2(\mathcal{T}_h)} \leq C \, h^{k+1},$$

where u_h is the approximation given by the DG method using polynomials of degree k, and $\partial_{\boldsymbol{\beta},h} u_h$ is an approximation to $\partial_{\boldsymbol{\beta}} u = \boldsymbol{\beta} \cdot \nabla u$ obtained by using an element-by-element postprocessing of u_h.

The special triangulations $\mathcal{T}_h$ for which the above result holds are strongly related to the transport velocity as follows. They are made of simplexes K satisfying three *flow* conditions. To state them, we need to introduce some notation. We say that a face e of the simplex K is interior if it is not included in $\partial\Omega$. We say that the face is an outflow (inflow) face (with respect to $\boldsymbol{\beta}$) if $\boldsymbol{\beta} \cdot \boldsymbol{n}_K|_e > \ (<) \ 0$. We also say that the face is almost parallel to $\boldsymbol{\beta}$ if

$$(1.2) \qquad \frac{1}{|e|} | \, \langle \boldsymbol{\beta} \cdot \boldsymbol{n}, 1 \rangle_e \, | \leq C_{\boldsymbol{\beta}} \, h_K$$

for some constant $C_{\boldsymbol{\beta}}$, where $h_K = diam(K)$.

We can now state the flow conditions on the triangulation. They are as follows:

(1.3a)   Each simplex K has at least one *outflow* face, one of which we denote by e_K^+.

(1.3b)   Each interior face e_K^+ is included in an *inflow* face of another simplex.

To state the third condition, we need to introduce some notation. We define $\mathscr{E}_h^+$ as the union of the faces e_K^+ for all simplexes $K \in \mathcal{T}_h$, $\mathscr{E}_h^o$ as the union of all faces e of the simplexes $K \in \mathcal{T}_h$ not in the set $\mathscr{E}_h^+$ and almost parallel to $\boldsymbol{\beta}$, and $\mathscr{E}_h^c$ as the union of all faces e of the simplexes $K \in \mathcal{T}_h$ not in $\mathscr{E}_h^+ \cup \mathscr{E}_h^o \cup \Gamma^-$. Note that $\mathscr{E}_h^+$ does not contain all outflow faces since there might be outflow faces lying on $\mathscr{E}_h^o$ or in $\mathscr{E}_h^c$; see Figure 1 for an illustration. With this notation, the third condition reads as follows:

$$(1.3c) \qquad \sum_{e \subset \mathscr{E}_h^c} |e|^{\frac{d-2}{d-1}} \leq C_c$$

for some constant C_c.

The above conditions extend the conditions satisfied by the special triangulations introduced in [6] for the case in which the velocity $\boldsymbol{\beta}$ is constant. Indeed, therein, the first condition required that the outflow face e_K^+ be unique. Moreover, almost parallel faces were not considered, and finally, the third condition was tacitly assumed to hold with $C_c = 0$ since $\boldsymbol{\beta} \cdot \boldsymbol{n}$ was equal to zero on any face e which was not e_K^+ or an inflow face.

Our analysis shows that it is not necessary to require such stringent conditions. Instead of the strictly parallel faces considered in [6], we can now consider almost parallel faces, that is, faces on which the *average* on e of the normal component of the transport velocity is *small* enough. This condition is not difficult to satisfy. It holds, for example, that when on the face e,

$$| \boldsymbol{\beta} \cdot \boldsymbol{n} | \leq C_{\boldsymbol{\beta}} \, h_K.$$

It also holds when $\boldsymbol{\beta} \cdot \boldsymbol{n}(\boldsymbol{x}_0) = 0$ for *any* particular point $\boldsymbol{x}_0$ of the face e. Indeed, since

$$\langle \boldsymbol{\beta} \cdot \boldsymbol{n}, 1 \rangle_e = \langle \boldsymbol{\beta} \cdot \boldsymbol{n} - \boldsymbol{\beta} \cdot \boldsymbol{n}(\boldsymbol{x}_0), 1 \rangle_e,$$
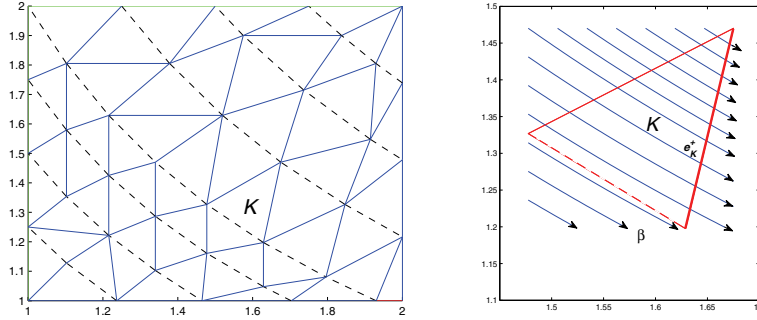
FIG. 1. *The figure on the left is a triangulation satisfying the flow conditions with $\boldsymbol{\beta} = (x, -y)$. The inflow boundary Γ^- is the union of $[1, 2] \times \{2\}$ and $\{1\} \times [1, 2]$, the set of faces $\mathscr{E}_h^+$ is marked with a solid line, the set of almost parallel faces $\mathscr{E}_h^o$ is marked with a dashed line, and the set $\mathscr{E}_h^c$ consists of only one edge, namely, the horizontal edge ending at the vertex $(2, 1)$. The figure on the right is a zoom of a single triangle K in the middle of the triangulation. The outflow edge e_K^+ is marked with a bold line and the edge that is almost parallel to $\boldsymbol{\beta}$ is marked with a dashed line.*

we have that

$$\frac{1}{|e|} |\langle \boldsymbol{\beta} \cdot \boldsymbol{n}, 1 \rangle_e | \le |\boldsymbol{\beta}|_{\boldsymbol{W}^{1,\infty}(e)} h_K,$$

and the third condition is satisfied with $C_{\boldsymbol{\beta}} := |\boldsymbol{\beta}|_{\boldsymbol{W}^{1,\infty}(\Omega)}$.

Let us now discuss the third condition, (1.3c). This condition allows us to work with triangulations containing simplexes with more than one outflow face. These simplexes can be anywhere in the domain. However, for the algorithm we propose to construct the triangulations (see section 3 on numerical experiments); these simplexes are typically those having more than one outflow face on the boundary of the domain Ω. In the two-dimensional case $d = 2$, the triangles having more than one edge on the boundary are those containing a vertex of Ω. All of these triangles are allowed by condition (1.3c) if we take C_c to be bigger than the number of vertices of the polygon Ω. Similarly, in the three-dimensional case $d = 3$, the tetrahedra having more than one face on the boundary of Ω are those having at least one edge lying on the edges of Ω. All of these tetrahedra can be allowed by condition (1.3c). Indeed, since $|e|^{\frac{d-2}{d-1}} = |e|^{\frac{1}{2}} \approx h_K$, it is enough to take C_c to be an upper bound of the sum of the length of the edges of Ω. This shows that condition (1.3c) is quite reasonable.

Of course, the families of triangulations we consider also satisfy the classical assumption of shape regularity; see [3]. Thus, there is a constant $\sigma > 0$ such that

(1.4)   for each simplex $K \in \mathcal{T}_h : h_K/\rho_K \ge \sigma,$

where h_K denotes the diameter of the simplex K and ρ_K the diameter of the biggest ball included in K.

The paper is organized as follows. In section 2 we state and prove our main results and, in section 3, we carry out numerical experiments validating them. We end in section 4 with some concluding remarks.

2. The main results.

2.1. The DG method.
Let us introduce the original DG method for our problem (1.1). Suppose we have a family of triangulations $\{\mathcal{T}_h\}$ of Ω satisfying the flow

conditions (1.3). To each triangulation $\mathcal{T}_h$, we associate the number $h = \sup_{K \in \mathcal{T}_h} h_K$, where $h_K = diam(K)$, and the finite-dimensional space V_h^k, which is composed of functions that are polynomials of degree at most k on each simplex $K \in \mathcal{T}_h$. Then, the DG approximation $u_h \in V_h$ of the solution of (1.1) is defined as the solution of

$$(2.1a) \qquad B(u_h, v_h) = (f, v_h)_{\mathcal{T}_h} - \langle g, v_h \, \boldsymbol{\beta} \cdot \boldsymbol{n} \rangle_{\Gamma^-} \quad \text{for all } v_h \in V_h,$$

where

$$(2.1b) \qquad B(w, v) := - (w, \partial_{\boldsymbol{\beta}} v)_{\mathcal{T}_h} + \langle \widehat{w}, v \, \boldsymbol{\beta} \cdot \boldsymbol{n} \rangle_{\partial \mathcal{T}_h \backslash \Gamma^-} + (c \, w, v)_{\mathcal{T}_h}$$

for any w, v in $H^1(\mathcal{T}_h)$. Here, the numerical trace of a function w on a point $z \in \partial K$ for a simplex $K \in \mathcal{T}_h$ is given by

$$(2.1c) \qquad\qquad\qquad \widehat{w} := w^-,$$

where $w^\pm(z) = \lim_{\delta \downarrow 0} w(z \pm \delta \boldsymbol{\beta}(z))$, where $z \in e$. We are using the notation

$$(\boldsymbol{\sigma}, \boldsymbol{v})_{\mathcal{T}_h} := \sum_{K \in \mathcal{T}_h} \int_K \boldsymbol{\sigma}(x) \cdot \boldsymbol{v}(x) \, dx, \qquad (\zeta, \omega)_{\mathcal{T}_h} := \sum_{K \in \mathcal{T}_h} \int_K \zeta(x) \, \omega(x) \, dx,$$

$$\langle \zeta, \boldsymbol{v} \cdot \boldsymbol{n} \rangle_{\partial \mathcal{T}_h} := \sum_{K \in \mathcal{T}_h} \int_{\partial K} \zeta(\gamma) \, \boldsymbol{v}(\gamma) \cdot \boldsymbol{n} \, d\gamma$$

for any functions $\boldsymbol{\sigma}, \boldsymbol{v}$ in $\boldsymbol{H}^1(\mathcal{T}_h) := [H^1(\mathcal{T}_h)]^d$ and ζ, ω in $H^1(\mathcal{T}_h)$. The outward normal unit vector to ∂K is denoted by $\boldsymbol{n}$.

Before we present our main result, we need to state the following stability result for the DG method. The following result is a simple consequence of the results found in [1].

LEMMA 2.1. *Suppose* (A1) *and* (A2) *hold, and assume that w_h satisfies $B(w_h, v) = F(v)$ for all $v \in V_h$, where F is a linear form. Then, for h sufficiently small,*

$$\|w_h\|_{L^2(\mathcal{T}_h)} \le C_s \max_{v \in V_h} \frac{|F(v)|}{\|v\|_{L^2(\mathcal{T}_h)}},$$

where C_s depends on the regularity of $\boldsymbol{\beta}$.

Of course, stability results like this are standard. For constant $\boldsymbol{\beta}$ the proof is in [11]. The case of variable $\boldsymbol{\beta}$, but imposing a stronger condition on the coefficients than (A1) and (A2), is contained in [9]. The above result is a simple consequence of the stability results given in [1]. For completeness, we sketch the proof of this lemma in the appendix.

2.2. The approximation of u. Our main result is the following.

THEOREM 2.2. *Suppose that the assumptions* (A1) *and* (A2) *hold. Assume also that the triangulation $\mathcal{T}_h$ satisfies the flow conditions* (1.3) *and the shape-regularity condition* (1.4). *Then, if h is small enough, we have*

$$\| u - u_h \|_{L^2(\mathcal{T}_h)} \le \mathsf{C} \, h^{k+1},$$

where $\mathsf{C} = C \, (1 + |\boldsymbol{\beta}|_{\boldsymbol{W}^{1,\infty}(\Omega)} + C_{\boldsymbol{\beta}}) \, | u |_{H^{k+1}(\mathcal{T}_h)} + C \, C_c^{1/2} \, \| \boldsymbol{\beta} \|_{L^\infty(\Omega)} \, | u |_{W^{k+1,\infty}(\mathcal{T}_h)}$ and C depends on C_s.

Note that this result is optimal in the order of convergence. It would also be optimal in the regularity of the exact solution if $C_c = 0$. This result is thus an extension of the corresponding result for the case of constant velocity in [6].

To prove the above estimate, we follow [6]. We proceed in several steps.

Step 1: *The projection* $\mathbb{P}$. We begin by recalling the definition of the projection $\mathbb{P}$, defined on triangulations $\mathcal{T}_h$ satisfying the flow condition (1.3a); see [5, 6]. The function $\mathbb{P}u \in V_h$ restricted to $K \in \mathcal{T}_h$ is given by

$$(2.2a) \qquad (\mathbb{P}u - u, v)_K = 0 \qquad \text{for all } v \in \mathcal{P}^{k-1}(K) \text{ if } k > 0,$$

$$(2.2b) \qquad \langle \mathbb{P}u - u, w \rangle_{e_K^+} = 0 \qquad \text{for all } w \in \mathcal{P}^k(e_K^+),$$

where $\mathcal{P}^\ell(D)$ stands for the space of polynomials of total degree at most ℓ defined on the set D. This projection can be considered as an extension to the multidimensional case of the projection used in [20] to study the one-dimensional case; see also [18] and [19]. In [8], a related projection is used to analyze DG methods for multidimensional linear, symmetric hyperbolic systems.

Since we have that

$$\|u - u_h\|_{L^2(\mathcal{T}_h)} \leq \|u - \mathbb{P}u\|_{L^2(\mathcal{T}_h)} + \|\mathbb{E}\|_{L^2(\mathcal{T}_h)},$$

where $\mathbb{E} = u_h - \mathbb{P}u$, if we assume the shape-regularity condition (1.4) on the triangulation $\mathcal{T}_h$, we have that (see [6])

$$\|\mathbb{P}u - u\|_{L^2(K)} \leq Ch^{k+1}|u|_{H^{k+1}(K)}.$$

Therefore, we have that

$$\|u - u_h\|_{L^2(\mathcal{T}_h)} \leq C|u|_{H^{k+1}(\mathcal{T}_h)} h^{k+1} + \|\mathbb{E}\|_{L^2(\mathcal{T}_h)}$$

whenever $u \in H^{k+1}(\mathcal{T}_h)$. It remains to estimate the projection of the error $\mathbb{E}$.

Step 2: *Estimate of* $\mathbb{E}$. By the error equation

$$B(u - u_h, v) = 0 \qquad \text{for all } v \in V_h,$$

and so, for all $v \in V_h$, we have that

$$B(\mathbb{E}, v) = B(u - \mathbb{P}u, v) = \sum_{i=1}^{3} T_i(v),$$

where, by definition of the bilinear form $B(\cdot, \cdot)$, (2.1b),

$$T_1(v) := -(u - \mathbb{P}u, \boldsymbol{\beta} \cdot \nabla v)_{\mathcal{T}_h},$$
$$T_2(v) := \langle u - \widehat{\mathbb{P}u}, v\,\boldsymbol{\beta} \cdot \boldsymbol{n} \rangle_{\partial \mathcal{T}_h \setminus \Gamma^-},$$
$$T_3(v) := (c\,(u - \mathbb{P}u), v)_{\mathcal{T}_h}.$$

Thus, by Lemma 2.1, we obtain

$$\|\mathbb{E}\|_{L^2(\mathcal{T}_h)} \leq C_s \sum_{i=1}^{3} \sup_{v \in V_h} \frac{|T_i(v)|}{\|v\|_{L^2(\mathcal{T}_h)}}$$

for h small enough.

It remains to estimate the linear forms $T_i(v)$, $i = 1, 2, 3$. To do that, we are going to use the auxiliary vector-valued function $\boldsymbol{\beta}^o$ defined as follows. On each simplex $K \in \mathcal{T}_h$, $\boldsymbol{\beta}^o$ is a constant vector defined by

$$(2.3) \qquad\qquad \langle (\boldsymbol{\beta} - \boldsymbol{\beta}^o) \cdot \boldsymbol{n}, 1 \rangle_e = 0$$

for all faces e of K except for *one* arbitrarily chosen face which is not the outflow face e_K^+ of the simplex K.

   Step 3: *Estimate of* T_1. Let us estimate $T_1(v)$. We have

$$T_1(v) = -(u - \mathbb{P}u, (\boldsymbol{\beta} - \boldsymbol{\beta}^o) \cdot \nabla v)_{\mathcal{T}_h},$$

by the definition of the projection $\mathbb{P}$, (2.2a), and by the definition of $\boldsymbol{\beta}^o$. This implies that

$$|T_1(v)| \leq \sum_{K \in \mathcal{T}_h} \| u - \mathbb{P}u \|_{L^2(K)} \| \boldsymbol{\beta} - \boldsymbol{\beta}^o \|_{\boldsymbol{L}^\infty(K)} \| \nabla v \|_{L^2(K)},$$

and, by a standard inverse inequality, that

$$\begin{aligned}
|T_1(v)| &\leq \sum_{K \in \mathcal{T}_h} \| u - \mathbb{P}u \|_{L^2(K)} \| \boldsymbol{\beta} - \boldsymbol{\beta}^o \|_{\boldsymbol{L}^\infty(K)} C_K h_K^{-1} \| v \|_{L^2(K)} \\
&\leq C \max_{K \in \mathcal{T}_h} \{ h_K^{-1} \| \boldsymbol{\beta} - \boldsymbol{\beta}^o \|_{\boldsymbol{L}^\infty(K)} \} \| u - \mathbb{P}u \|_{L^2(\mathcal{T}_h)} \| v \|_{L^2(\mathcal{T}_h)} \\
&\leq C | \boldsymbol{\beta} |_{\boldsymbol{W}^{1,\infty}(\mathcal{T}_h)} \| u - \mathbb{P}u \|_{L^2(\mathcal{T}_h)} \| v \|_{L^2(\mathcal{T}_h)} \\
&\leq C | \boldsymbol{\beta} |_{\boldsymbol{W}^{1,\infty}(\mathcal{T}_h)} h^{k+1} | u |_{H^{k+1}(\mathcal{T}_h)} \| v \|_{L^2(\mathcal{T}_h)},
\end{aligned}$$

by the approximation properties of $\boldsymbol{\beta}^0$ (see [4]), the shape-regularity assumption on the mesh (1.4), and by the approximation properties of $\mathbb{P}$; see [6].

   Step 4: *Estimate of* T_2. Let us now estimate $T_2(v)$. We begin by writing $T_2(v)$ as

$$T_2(v) = U_1(v) + U_2(v),$$

where

$$\begin{aligned}
U_1(v) &= \sum_{K \in \mathcal{T}_h} \langle u - \widehat{\mathbb{P}u}, v \, (\boldsymbol{\beta} - \boldsymbol{\beta}^o) \cdot \boldsymbol{n} \rangle_{\partial K \setminus \Gamma^-}, \\
U_2(v) &= \sum_{K \in \mathcal{T}_h} \langle u - \widehat{\mathbb{P}u}, v \, \boldsymbol{\beta}^o \cdot \boldsymbol{n} \rangle_{\partial K \setminus \Gamma^-}.
\end{aligned}$$

Next, let us estimate $U_1(v)$. We have

$$\begin{aligned}
|U_1(v)| &\leq \sum_{K \in \mathcal{T}_h} \| u - \widehat{\mathbb{P}u} \|_{L^2(\partial K)} \| v \|_{L^2(\partial K)} \| (\boldsymbol{\beta} - \boldsymbol{\beta}^o) \cdot \boldsymbol{n} \|_{L^\infty(\partial K)} \\
&\leq \sum_{K \in \mathcal{T}_h} C_K h_K^{k+1/2} | u |_{H^{k+1}(K)} \| v \|_{L^2(\partial K)} h_K | \boldsymbol{\beta} |_{\boldsymbol{W}^{1,\infty}(\partial K)}
\end{aligned}$$

by the approximation properties of $\mathbb{P}$ and $\boldsymbol{\beta}^o$. Then, after applying a simple inverse inequality, we get

$$|U_1(v)| \leq C | \boldsymbol{\beta} |_{\boldsymbol{W}^{1,\infty}(\Omega)} h^{k+1} | u |_{H^{k+1}(\mathcal{T}_h)} \| v \|_{L^2(\mathcal{T}_h)}.$$

Let us estimate $U_2(v)$. To do that, we rewrite $U_2(v)$ as

$$U_2(v) = S_1(v) + S_2(v) + S_3(v),$$

where

$$S_1(v) = \sum_{K \in \mathcal{T}_h} \langle u - \widehat{\mathbb{P}u}, v\, \boldsymbol{\beta}^o \cdot \boldsymbol{n} \rangle_{(\partial K \cap \mathscr{E}_h^+) \backslash \Gamma^-},$$

$$S_2(v) = \sum_{K \in \mathcal{T}_h} \langle u - \widehat{\mathbb{P}u}, v\, \boldsymbol{\beta}^o \cdot \boldsymbol{n} \rangle_{(\partial K \cap \mathscr{E}_h^o) \backslash \Gamma^-},$$

$$S_3(v) = \sum_{K \in \mathcal{T}_h} \langle u - \widehat{\mathbb{P}u}, v\, \boldsymbol{\beta}^o \cdot \boldsymbol{n} \rangle_{(\partial K \cap \mathscr{E}_h^c) \backslash \Gamma^-}.$$

Let us recall that $\mathscr{E}_h^+$ is the union of faces e_K^+ for all $K \in \mathcal{T}_h$, $\mathscr{E}_h^o$ the union of all faces not in $\mathscr{E}_h^+$ which are almost parallel to $\boldsymbol{\beta}$, and $\mathscr{E}_h^c$ the union of all faces which are not in $\mathscr{E}_h^+ \cup \mathscr{E}_h^o \cup \Gamma^-$.

Let us begin by estimating $S_1(v)$. By the first flow condition on the mesh (1.3a), it follows that

$$S_1(v) = \sum_{K \in \mathcal{T}_h} \langle u - \widehat{\mathbb{P}u}, (v^- - v^+)\boldsymbol{\beta}^o \cdot \boldsymbol{n} \rangle_{e_K^+ \backslash \Gamma^+} + \sum_{K \in \mathcal{T}_h} \langle u - \widehat{\mathbb{P}u}, v\, \boldsymbol{\beta}^o \cdot \boldsymbol{n} \rangle_{e_K^+ \cap \Gamma^+}.$$

Note that here we have used in an essential manner that the normal component of the auxiliary function $\boldsymbol{\beta}^o$ across the outflow faces e_K^+ is single valued; this is guaranteed by the definition of $\boldsymbol{\beta}^o$, (2.3). Now, by the definition of the numerical trace $\widehat{\mathbb{P}u}$, (2.1), we obtain that

$$S_1(v) = \sum_{K \in \mathcal{T}_h} \langle u - \mathbb{P}u, (v^- - v^+)\boldsymbol{\beta}^o \cdot \boldsymbol{n} \rangle_{e_K^+ \backslash \Gamma^+} + \sum_{K \in \mathcal{T}_h} \langle u - \mathbb{P}u, v\, \boldsymbol{\beta}^o \cdot \boldsymbol{n} \rangle_{e_K^+ \cap \Gamma^+}.$$

But, by the second flow condition on the mesh (1.3b), the function $(v^- - v^+)\boldsymbol{\beta}^o \cdot \boldsymbol{n}|_{e_K^+}$ belongs to $\mathcal{P}^k(e_K^+)$, and we can conclude that, by the definition of the projection $\mathbb{P}$, (2.2b),

$$S_1(v) = 0.$$

Next, let us estimate $S_2(v)$. We have

$$|S_2(v)| \leq \sum_{K \in \mathcal{T}_h} \|u - \widehat{\mathbb{P}u}\|_{L^2(\partial K \cap \mathscr{E}_h^o)} \|v\|_{L^2(\partial K \cap \mathscr{E}_h^o)} \|\boldsymbol{\beta}^o \cdot \boldsymbol{n}\|_{L^\infty(\partial K \cap \mathscr{E}_h^o)},$$

and since all the faces e in $\mathscr{E}_h^o$ satisfy condition (1.2),

$$|S_2(v)| \leq \sum_{K \in \mathcal{T}_h} \|u - \widehat{\mathbb{P}u}\|_{L^2(\partial K \cap \mathscr{E}_h^o)} \|v\|_{L^2(\partial K \cap \mathscr{E}_h^o)} C_{\boldsymbol{\beta}}\, h_K$$

$$\leq C\, C_{\boldsymbol{\beta}}\, h^{k+1}\, |u|_{H^{k+1}(\mathcal{T}_h)} \|v\|_{L^2(\mathcal{T}_h)}.$$

It remains to estimate $S_3(v)$. We have

$$| S_3(v) | \leq \| u - \widehat{\mathbb{P}u} \|_{L^\infty(\mathscr{E}_h^c)} \| \boldsymbol{\beta}^o \|_{L^\infty(\mathscr{E}_h^c)} \sum_{K \in \mathfrak{T}_h} \| v \|_{L^1(\partial K \cap \mathscr{E}_h^c)}$$

$$\leq C h^{k+1} | u |_{W^{k+1,\infty}(\mathfrak{T}_h)} \| \boldsymbol{\beta} \|_{L^\infty(\Omega)} \sum_{K \in \mathfrak{T}_h} \| v \|_{L^1(\partial K \cap \mathscr{E}_h^c)}$$

by the approximation properties of the projection $\mathbb{P}$ and the definition of $\boldsymbol{\beta}^o$. Next, note that, by a scaling argument, we have

$$\sum_{K \in \mathfrak{T}_h} \| v \|_{L^1(\partial K \cap \mathscr{E}_h^c)} \leq C \sum_{K \in \mathfrak{T}_h} \| v \|_{L^2(K)} h_K^{-d/2} |\partial K \cap \mathscr{E}_h^c|$$

$$\leq C \| v \|_{\mathfrak{T}_h} \left(\sum_{K \in \mathfrak{T}_h} h_K^{-d} |\partial K \cap \mathscr{E}_h^c|^2 \right)^{1/2}$$

$$\leq C \| v \|_{\mathfrak{T}_h} \left(\sum_{e \in \mathscr{E}_h^c} |e|^{-\frac{d}{d-1}} |e|^2 \right)^{1/2}$$

$$\leq C C_c^{1/2} \| v \|_{\mathfrak{T}_h}$$

by the third condition on the triangulation (1.3c). This implies that

$$| S_3(v) | \leq C C_c^{1/2} h^{k+1} | u |_{W^{k+1,\infty}(\mathfrak{T}_h)} \| \boldsymbol{\beta} \|_{L^\infty(\Omega)} \| v \|_{\mathfrak{T}_h}.$$

As a consequence, we obtain

$$| T_2(v) | \leq C(C_{\boldsymbol{\beta}} + | \boldsymbol{\beta} |_{\boldsymbol{W}^{1,\infty}(\Omega)}) | u |_{H^{k+1}(\mathfrak{T}_h)} \| v \|_{L^2(\mathfrak{T}_h)}$$
$$+ C C_c^{1/2} \| \boldsymbol{\beta} \|_{L^\infty(\Omega)} h^{k+1} | u |_{W^{k+1,\infty}(\mathfrak{T}_h)} \| v \|_{L^2(\mathfrak{T}_h)}.$$

Step 5: *Estimate of T_3.* A simple application of the Cauchy–Schwarz inequality gives

$$| T_3(v) | \leq \| c (u - \mathbb{P}u) \| \| v \|_{L^2(\mathfrak{T}_h)}$$
$$\leq C | u |_{H^{k+1}(\mathfrak{T}_h)} h^{k+1} \| v \|_{L^2(\mathfrak{T}_h)}$$

by the approximation properties of $\mathbb{P}$.

Step 6: *Conclusion.* We have

$$\| u - u_h \|_{L^2(\mathfrak{T}_h)} \leq C | u |_{H^{k+1}(\mathfrak{T}_h)} h^{k+1} + \| \mathbb{E} \|_{L^2(\mathfrak{T}_h)} \qquad \text{(by Step 1)}$$

$$\leq C | u |_{H^{k+1}(\mathfrak{T}_h)} h^{k+1} + C_s \sum_{i=1}^3 \sup_{v \in V_h} \frac{| T_i(v) |}{\| v \|_{L^2(\mathfrak{T}_h)}} \qquad \text{(by Step 2)}$$

$$\leq C (1 + | \boldsymbol{\beta} |_{\boldsymbol{W}^{1,\infty}(\Omega)} + C_{\boldsymbol{\beta}}) h^{k+1} | u |_{H^{k+1}(\mathfrak{T}_h)}$$
$$+ C C_c^{1/2} \| \boldsymbol{\beta} \|_{L^\infty(\Omega)} h^{k+1} | u |_{W^{k+1,\infty}(\mathfrak{T}_h)}$$

by Steps 3, 4, and 5. This completes the proof of Theorem 2.2.

2.3. Postprocessing: The approximation to $\partial_{\boldsymbol{\beta}} u$. Next we postprocess u_h to get a superconvergent approximation of $\partial_{\boldsymbol{\beta}} u$. We follow [6], and for each simplex K we define $\boldsymbol{q}_h \in \boldsymbol{\mathcal{P}}^k(K) + \boldsymbol{x}\,\mathcal{P}^k(K)$ to be the solution of

$$(2.4a) \qquad (\boldsymbol{q}_h - \boldsymbol{\beta} u_h, \boldsymbol{v})_K = 0 \qquad \text{for all } \boldsymbol{v} \in \boldsymbol{\mathcal{P}}^{k-1}(K) \text{ if } k > 0,$$

$$(2.4b) \qquad \langle (\boldsymbol{q}_h - \boldsymbol{\beta}\lambda_h) \cdot \boldsymbol{n}, w \rangle_e = 0 \qquad \text{for all } w \in \mathcal{P}^k(e), \text{ for all faces } e \text{ of } K,$$

where $\lambda_h = \mathsf{P}_{\partial} g$ on Γ^- and $\lambda_h = \widehat{u}_h$ otherwise; here $\boldsymbol{\mathcal{P}}^k(K) := [\mathcal{P}^k(K)]^d$. The existence and uniqueness of $\boldsymbol{q}_h$ is well known; see, for example, [2]. We then define

$$\partial_{\boldsymbol{\beta},h} u_h := \nabla \cdot \boldsymbol{q}_h - u_h \nabla \cdot \boldsymbol{\beta} \qquad \text{in } \mathcal{T}_h.$$

We can now state the error estimate between $\partial_{\boldsymbol{\beta},h} u_h$ and $\partial_{\boldsymbol{\beta}} u$.

THEOREM 2.3. *Suppose that the assumptions* (A1) *and* (A2) *hold. Assume also that the triangulation $\mathcal{T}_h$ satisfies the flow conditions* (1.3) *and the shape-regularity condition* (1.4). *Then, if h is small enough, we have*

$$\|\partial_{\boldsymbol{\beta},h} u_h - \mathsf{P}(\partial_{\boldsymbol{\beta}} u)\|_{L^2(\mathcal{T}_h)} \leq C\,\mathsf{C}\,h^{k+1}.$$

Proof. Following exactly the same argument used in [6], we obtain that

$$(\nabla \cdot (\boldsymbol{q} - \boldsymbol{q}_h), v_h)_{\mathcal{T}_h} = (c(u_h - u), v_h)_{\mathcal{T}_h}$$

for all $v_h \in V_h$. This readily implies that

$$(\partial_{\boldsymbol{\beta}} u - \partial_{\boldsymbol{\beta},h} u_h, v_h)_{\mathcal{T}_h} = ((c + \nabla \cdot \boldsymbol{\beta})(u_h - u), v_h)_{\mathcal{T}_h}$$

for all $v_h \in V_h$, and so, if $\mathcal{T}_h$ is an *arbitrary*, shape-regular triangulation of Ω, we have

$$\|\partial_{\boldsymbol{\beta},h} u_h - \mathsf{P}(\partial_{\boldsymbol{\beta}} u)\|_{L^2(\mathcal{T}_h)} \leq C\,\|\,u - u_h\,\|_{L^2(\mathcal{T}_h)}.$$

Then, for the special triangulation $\mathcal{T}_h$ under consideration, we get that

$$\|\partial_{\boldsymbol{\beta},h} u_h - \mathsf{P}(\partial_{\boldsymbol{\beta}} u)\|_{L^2(\mathcal{T}_h)} \leq C\,\mathsf{C}\,h^{k+1}$$

by Theorem 2.2. This completes the proof. ☐

3. Numerical results. In this section we present two numerical experiments to validate our theoretical results. We describe the test problems and then the algorithm we use to generate triangulations satisfying the flow conditions. Finally, we display and discuss the history of convergence of the method for each of the two above-mentioned problems.

The test problems. Physically, the model equation (1.1) describes transport-reaction phenomena including neutron transport and radiative transfer. Our first example is from geometrical optics where the model equation is the so-called Liouville equation; in this case, the velocity $\boldsymbol{\beta}$ is divergence-free. In the second example, we take a velocity $\boldsymbol{\beta}$ whose divergence is not zero.

In geometrical optics for wave propagation, we need to solve the Liouville equations efficiently and accurately to be able to compute the multivalued traveltime and the amplitude; see [15, 7, 12]. In the case of acoustic waves, the Hamiltonian defining the Liouville operator has the form $H(x, y) = xy$; the resulting velocity is $\boldsymbol{\beta}(x, y) = (H_y, -H_x) = (x, -y)$. This is our first test problem. Therefore, the

results presented here lay a theoretical foundation for developing fast and accurate algorithms for solving Liouville equations. In the numerical experiment, we take the domain $\Omega = [1, 2] \times [1, 2]$ and the reaction coefficient $c(x, y) = y$. The right-hand side f is chosen so that the solution is $u(x, y) = (x + 1/2)^3 \sin(y)$.

In the second test problem, we consider a nonlinear velocity $\beta(x, y) = ((x + 1)^2 (y + 1/2), (x + 1/10)(y + 1)^2)$ whose divergence is nonzero on the domain $[0, 1] \times [0, 1]$. We take the reaction coefficient $c(x, y) = \nabla \cdot \beta$. Then (1.1a) is equivalent to $\beta \cdot \nabla u = f$. Again, we choose the right-hand side f so that the solution is $u(x, y) = (x + 1/2)^3 \sin(y)$.

Generating the triangulations. We do not want to give a precise description of the algorithm to obtain triangulations satisfying the flow conditions (1.3). Instead, we just give the main idea to generate the triangulation:

(i) Given a positive number h, we triangulate the inflow boundary Γ^- in segments of size no bigger than h.

(ii) For each of the nodes $\boldsymbol{x}_0$ of Γ^-, we apply the forward Euler time-marching method to the problem

$$\frac{d}{dt}x(t) = \boldsymbol{\beta}(\boldsymbol{x}(t)) \quad t > 0, \quad \boldsymbol{x}(0) = \boldsymbol{x}_0,$$

to obtain the set of nodes $\{\boldsymbol{x}_i\}_{i=1}^{N(\boldsymbol{x}_0)}$ such that the distance between $\boldsymbol{x}_i$ and $\boldsymbol{x}_{i-1}$ is of order h and $\boldsymbol{x}_N(\boldsymbol{x}_0)$ is the point on the outflow boundary.

(iii) We add the vertices of the outflow boundary to the set of nodes. Then we generate a triangulation.

(iv) We numerically check the flow conditions and modify the simplexes which violate the flow conditions by using an algorithm similar to that in [10].

For both of the problems under consideration, we have used the above idea to generate the triangulations. Examples of the meshes are displayed in Figures 2 and 3. We have numerically checked the flow conditions on each of the meshes by computing the sign of $\boldsymbol{\beta} \cdot \boldsymbol{n}$ on equally spaced points on each edge, numerically integrating $\boldsymbol{\beta} \cdot \boldsymbol{n}$ on edges which are not inflow, and testing the condition (1.2) with $C_{\boldsymbol{\beta}} = \|\boldsymbol{\beta}\|_{\boldsymbol{W}^{1,\infty}(\Omega)}$. Note that the triangles containing a vertex of the outflow boundary could have two outflow boundaries, which is allowed by the third flow condition (1.3c).
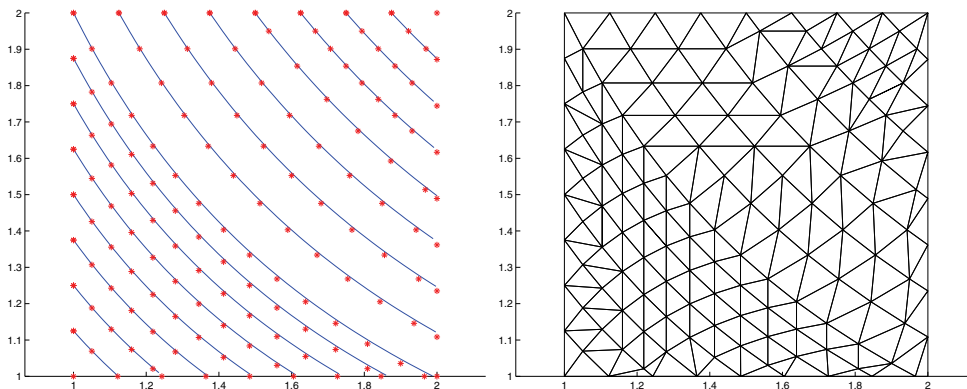

FIG. 2. *Meshes satisfying the flow condition with respect to $\boldsymbol{\beta} = (x, -y)$: The streamlines of β and the nodes of the mesh (left) and the actual mesh ($\ell = 3$) (right).*
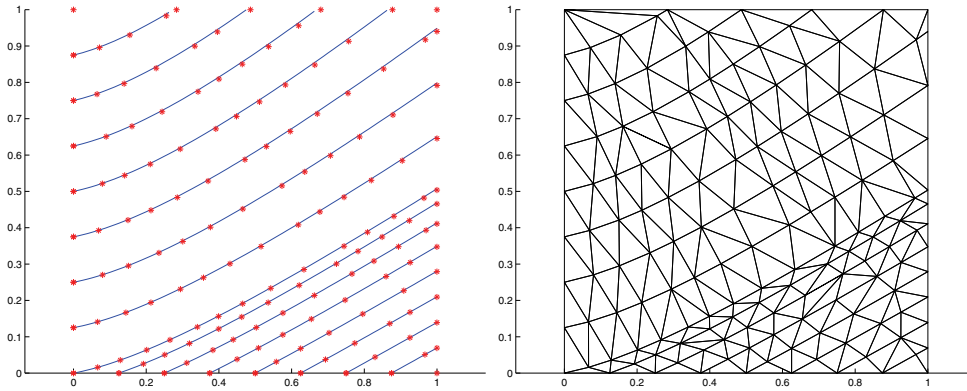
FIG. 3. *Meshes satisfying the flow condition with respect to* $\boldsymbol{\beta} = ((x+1)^2(y+1/2), (x+1/10)(y+1)^2)$: *The streamlines of* β *and the nodes of the mesh (left) and the actual mesh* $(\ell = 3)$ *(right).*

TABLE 3.1
History of convergence for the acoustic waves problem.

	mesh	$\|u - u_h\|_{L^2(\Omega)}$		$\|\partial_{\boldsymbol{\beta}} u - \partial_{\boldsymbol{\beta},h} u_h\|_{L^2(\Omega)}$	
k	ℓ	error	order	error	order
	1	.11e+1	–	.26e+1	–
	2	.49e−0	1.21	.12e+1	1.12
0	3	.24e−0	0.99	.61e−0	1.01
	4	.13e−0	0.96	.31e−0	0.98
	5	.63e−1	0.99	.15e−0	0.99
	1	.71e−1	–	.17e−0	–
	2	.15e−1	2.29	.37e−1	2.24
1	3	.38e−2	1.96	.92e−2	2.00
	4	.99e−3	1.93	.24e−2	1.94
	5	.25e−3	1.99	.60e−3	2.00
	1	.30e−2	–	.60e−2	–
	2	.37e−3	3.02	.66e−3	3.18
2	3	.48e−4	2.96	.83e−4	2.97
	4	.60e−5	2.99	.11e−4	2.98
	5	.76e−6	3.00	.14e−5	2.92

The history of convergence. In the first numerical experiment, the convection velocity is $\boldsymbol{\beta}(x, y) = (x, -y)$, which is divergence-free. The nodes of the meshes are close to the streamlines of $\boldsymbol{\beta}$, as seen in Figure 2 (left). Note that the nodes do not have to lie exactly on the streamlines; see, for example, the nodes near the outflow corner point $(2,1)$ in Figure 2 (left). Note also that the triangle at the outflow corner $(2,1)$ has two outflow edges in Figure 2 (right); this is allowed by the flow condition (1.3c). We have numerically checked that the three conditions on the mesh (1.3) are satisfied; see Figure 2 (right).

In Table 3.1, we display the history of convergence for the approximate solution using polynomials of degree $k = 0, 1, 2$. Therein, the parameter ℓ is associated with the mesh $h := 1/2^\ell$. We see that the order $k + 1$ is observed for both $\|u - u_h\|_{L^2(\Omega)}$ and $\|\partial_{\boldsymbol{\beta}} u - \partial_{\boldsymbol{\beta},h} u_h\|_{L^2(\Omega)}$, just as the theory predicts.

TABLE 3.2
History of convergence for the nondivergence-free velocity.

	mesh	$\|u - u_h\|_{L^2(\Omega)}$		$\|\partial_{\boldsymbol{\beta}} u - \partial_{\boldsymbol{\beta},h} u_h\|_{L^2(\Omega)}$	
k	ℓ	error	order	error	order
	1	.35e−0	–	.29e+1	–
	2	.17e−0	1.06	.14e+1	1.01
0	3	.80e−1	1.09	.71e−0	1.02
	4	.40e−1	1.00	.36e−0	0.96
	5	.20e−1	0.99	.18e−0	0.99
	1	.35e−1	–	.61e−0	–
	2	.75e−2	2.20	.13e−0	2.20
1	3	.17e−2	2.11	.30e−1	2.13
	4	.43e−3	2.00	.79e−2	1.94
	5	.11e−3	2.01	.19e−2	2.02
	1	.22e−2	–	.79e−2	–
	2	.24e−3	3.20	.73e−3	3.43
2	3	.28e−4	3.08	.78e−4	3.22
	4	.33e−5	3.06	.98e−5	3.00
	5	.40e−6	3.05	.11e−5	3.13

In the second numerical experiment, we take the convection coefficient to be $\boldsymbol{\beta}(x, y) = ((x + 1)^2(y + 1/2), (x + 1/10)(y + 1)^2)$, which is non–divergence-free on the domain $[0, 1] \times [0, 1]$. Similarly, the nodes of the meshes are obtained by numerically tracing the streamlines of $\boldsymbol{\beta}$ with the forward Euler method; see Figure 3 (left). Note that even though the nodes near the outflow corner point (1,0) are not exactly on the streamlines in Figure 3 (left), the three conditions on the mesh (1.3) are satisfied; see Figure 3 (right).

In Table 3.2, we display the history of convergence for the approximate solution using polynomials of degree $k = 0, 1, 2$. We see that the order $k + 1$ is observed for $\|u - u_h\|_{L^2(\Omega)}$ and $\|\partial_{\boldsymbol{\beta}} u - \partial_{\boldsymbol{\beta},h} u_h\|_{L^2(\Omega)}$, just as the theory predicts.

4. Concluding remarks. In this paper, we have uncovered a class of meshes for which the DG method converges in an optimal way, thus extending the results in [6] for constant transport velocities $\boldsymbol{\beta}$ to a large class of variable transport velocities. An idea for constructing these meshes in the two-dimensional case was sketched. For the three-dimensional case, a similar idea can be used together with the algorithm for constructing the special meshes for constant velocities proposed in [6].

The extension of these results to curved-boundary domains Ω constitutes the subject of ongoing work.

Appendix: Sketch of Proof of Lemma 2.1. Ayuso and Marini [1] showed, assuming (A1) and (A2), that there exists a constant $c > 0$ such that for h sufficiently small

$$c \|v\|^2_{L^2(\mathcal{T}_h)} \leq B(v, \mathsf{P}(\varphi \, v)) \quad \text{for all } v \in V_h.$$

Here φ is a properly constructed function and P is the L^2-projection operator onto V_h. This result can be found on page 1406 of [1], where they use $a^{rc}(\cdot, \cdot)$ to denote the bilinear form $B(\cdot, \cdot)$. Note that in [1] they had more assumptions on the coefficients,

but this is because they considered the more complicated convection-reaction-diffusion problem. For the convection-reaction problem that we consider here, (A1) and (A2) are the only conditions that are needed.

Hence,

$$
\begin{aligned}
c\,\|w_h\|^2_{L^2(\mathcal{T}_h)} &\le B(w_h, \mathsf{P}(\varphi\,w_h)) \\
&= F(\mathsf{P}(\varphi\,w_h)) \\
&\le \|\mathsf{P}(\varphi\,w_h)\|_{L^2(\mathcal{T}_h)} \max_{v\in V_h} \frac{|F(v)|}{\|v\|_{L^2(\mathcal{T}_h)}} \\
&\le \|\varphi\,w_h\|_{L^2(\mathcal{T}_h)} \max_{v\in V_h} \frac{|F(v)|}{\|v\|_{L^2(\mathcal{T}_h)}} \\
&\le C\|w_h\|_{L^2(\mathcal{T}_h)} \max_{v\in V_h} \frac{|F(v)|}{\|v\|_{L^2(\mathcal{T}_h)}}.
\end{aligned}
$$

Here we used that φ is uniformly bounded independent of h, which follows from the construction of φ; see [1]. The result now follows by dividing both sides by $\|w_h\|_{L^2(\mathcal{T}_h)}$.

REFERENCES

[1] B. Ayuso and L. D. Marini, *Discontinuous Galerkin methods for advection-diffusion-reaction problems*, SIAM J. Numer. Anal., 47 (2009), pp. 1391–1420.

[2] F. Brezzi and M. Fortin, *Mixed and Hybrid Finite Element Methods*, Springer Ser. Comput. Math. 15, Springer-Verlag, New York, 1991.

[3] P. Ciarlet, *The Finite Element Method for Elliptic Problems*, North–Holland, Armsterdam, 1978.

[4] B. Cockburn and B. Dong, *An analysis of the minimal dissipation local discontinuous Galerkin method for convection-diffusion problems*, J. Sci. Comput., 32 (2007), pp. 233–262.

[5] B. Cockburn, B. Dong, and J. Guzmán, *A superconvergent LDG-hybridizable Galerkin method for second-order elliptic problems*, Math. Comp., 77 (2008), pp. 1887–1916.

[6] B. Cockburn, B. Dong, and J. Guzmán, *Optimal convergence of the original DG method for the transport-reaction equation on special meshes*, SIAM J. Numer. Anal., 46 (2008), pp. 1250–1265.

[7] B. Cockburn, J. Qian, F. Reitich, and J. Wang, *An accurate spectral/discontinuous finite-element formulation of a phase-space-based level set approach to geometrical optics*, J. Comput. Phys., 208 (2005), pp. 175–195.

[8] R. S. Falk and G. R. Richter, *Explicit finite element methods for symmetric hyperbolic equations*, SIAM J. Numer. Anal., 36 (1999), pp. 935–952.

[9] P. Houston, C. Schwab, and E. Süli, *Discontinuous hp-finite element methods for advection-diffusion-reaction problems*, SIAM J. Numer. Anal., 39 (2002), pp. 2133–2163.

[10] T. Iliescu, *A flow-aligning algorithm for convection-dominated problems*, Internat. J. Numer. Methods Engrg., 46 (1999), pp. 993–1000.

[11] C. Johnson and J. Pitkäranta, *An analysis of the discontinuous Galerkin method for a scalar hyperbolic equation*, Math. Comp., 46 (1986), pp. 1–26.

[12] S. Leung, J. Qian, and R. Burridge, *Eulerian Gaussian beams for high frequency wave propagation*, Geophysics, 72 (2007), pp. SM61–SM76.

[13] P. Lesaint and P. A. Raviart, *On a finite element method for solving the neutron transport equation*, in Mathematical Aspects of Finite Elements in Partial Differential Equations, C. de Boor, ed., Academic Press, New York, 1974, pp. 89–123.

[14] T. E. Peterson, *A note on the convergence of the discontinuous Galerkin method for a scalar hyperbolic equation*, SIAM J. Numer. Anal., 28 (1991), pp. 133–140.

[15] J. Qian and S. Leung, *A level set based Eulerian method for paraxial multivalued traveltimes*, J. Comput. Phys., 197 (2004), pp. 711–736.

[16] W. H. Reed and T. R. Hill, *Triangular Mesh Methods for the Neutron Transport Equation*, Technical report LA-UR-73- 479, Los Alamos Scientific Laboratory, Los Alamos, NM, 1973.

[17] G. R. Richter, *On the order of convergence of the discontinuous Galerkin method for hyperbolic equations*, Math. Comp., 77 (2008), pp. 1871–1885.

[18] D. Schötzau, *hp-DGFEM for Parabolic Evolution Problems—Applications to Diffusion and Viscous Incompressible Fluid Flow*, Ph.D. thesis, Dissertation 13041, Swiss Federal Institute of Technology, Zürich, Switzerland, 1999.

[19] D. Schötzau and C. Schwab, *Time discretization of parabolic problems by the hp-version of the discontinuous Galerkin finite element method*, SIAM J. Numer. Anal., 38 (2000), pp. 837–875.

[20] V. Thomée, *Galerkin Finite Element Methods for Parabolic Problems*, Springer Ser. Comput. Math. 25, Springer-Verlag, Berlin, 1997.